Electronic Supplementary Material (ESI) for Chemical Communications.

Supplementary Information

Redox-controlled δ-Dawson $\{Mn^{III}_2W_{17}\}$ polyoxometalate with photocatalytic H_2 evolution activity

Yan-Qing Jiao, Chao Qin, Xin-Long Wang*, Fu-Hong Liu, Peng Huang, Chun-Gang Wang, Kui-Zhan Shao and Zhong-Min Su*

Institute of Functional Material Chemistry, Key Lab of Polyoxometalate Science of Ministry of Education, Faculty of Chemistry, Northeast Normal University, Changchun 130024, P. R. China. Fax: +86-431-85684009; Tel: +86-431-85099108. E-mail: zmsu@nenu.edu.cn.

1. Materials and Measurements

All the chemicals were obtained from commercial sources, and were used without further purification. Elemental analyses (C, N, and H) were measured on a Perkin-Elmer 2400 CHN elemental analyzer; Mn and W were determined with a Plasma-SPEC(I) ICP atomic emission spectrometer. UV/Vis absorption spectra were obtained by using a 752 PC UV/Vis spectrophotometer. Diffuse reflectivity was measured from 200 to 800 nm using barium sulfate ($BaSO_4$) as a standard with 100% reflectance on a Varian Cary 500 UV-Vis spectrophotometer. Single-crystal X-ray diffraction data were recorded on a Bruker Apex CCD II area-detector diffractometer with graphite-monochromated Mo-Kα radiation (λ = 0.71069 Å) at 298(2) K. Absorption corrections were applied using multiscan technique and performed by using the SADABS program. The structure was solved by direct methods and refined on F^2 by full-matrix leastsquares methods by using the SHELXTL package. Powder X-ray diffraction measurement was recorded radiation ranging from 5º to 50º at room temperature on a Siemens D5005 diffractometer with Cu-Kα (λ = 1.5418 Å). Thermogravimetric analysis (TGA) of the samples was performed using a Perkin-Elmer TG-7 analyzer heated from room temperature to 600 ºC under nitrogen at the heating rate of 10 °C·min^{-1}. X-ray photoelectron spectroscopy analyses were performed on a VG ESCALABMKII spectrometer with an Al-Kα (1486.6 eV) achromatic X-ray source. The vacuum inside the analysis chamber was maintained at 6.2×10^{-6} Pa during the analysis. Magnetic susceptibilities were measured on finely grounded single crystal samples (grease restricted) with the use of a Quantum Design SQUID magnetometer MPMS-XL. Dynamic light scattering (DLS): DLS measurements were done by using a Zetasizer NanoZS (Malvern Instruments). Contact angles were measured on a KRÜSS DSA20MK2 Drop Shape Analysis System at 25°C. Electrospray ionization mass spectrometry was carried out with a Bruker Micro TOF-QII instrument. The electrochemical measurement was carried out on a CHI 660 electrochemical workstation at room temperature. The solutions were deaerated thoroughly for at least 30 min with pure nitrogen and kept under a positive pressure of this gas during the experiments. A conventional three-electrode system was employed to study the cyclic voltammetric behavior. The glass carbon electrode was used as a working electrode; Ag/AgCl as a reference electrode; Pt coil as a counter electrode, and the 0.5 mol·L^{-1} H_2SO_4 (pH = 0.33) solution was used as electrolyte. Photocatalytic reactions were carried out in a Pyrex inner-irradiation-type reaction vessel with a magnetic stirrer at room temperature. The reactant solution was

evacuated using N_2 several times to ensure complete air removal and then irradiated by using a 500 W mercury lamp. The produced H_2 was analyzed by a GC9800 instrument with a thermal conductivity detector and a 5 Å molecular sieve column (2 mm × 2 m) using N_2 as carrier gas.

2. Synthesis

Synthesis of **1**: A mixture of $Na_2WO_4 \cdot 2H_2O$ (2.0 g) and $NaOAc \cdot 3H_2O$ (8 g) in 40 mL of water was adjusted the pH to 2.6 with 2M HCl. And then Mn_{12}-acetate (0.5 g) was added to the solution in portions. The mixture was vigorously stirred at room temperature for 60 min, then refluxed at 100 °C for another 120 min, and filtered while hot. Dimethylamine hydrochloride (2.0 g) was added to the resulting filtrate, and the clear, brown solution was left to crystallize at room temperature. Rufous crystals suitable for X-ray crystallography were obtained after approximately two month (yield 6.3 mg, 38% based on W). Elemental analysis: Anal. Calc.: H 1.36; C 3.13; N 1.82; Cl 1.54; Mn 2.39; W 67.97 %. Found: H 1.38; C 3.16; N 1.76; Cl 1.31; Mn 2.44; W 67.21 %.

3. Crystallographic data for 1

Crystallographic data for **1** ($H_{62}C_{12}N_6O_{63}Cl_2Mn_2W_{17}$), Mr = 4604.62, orthorhombic, space group *Cmc2(1)*, a = 17.607(5) Å, b = 21.831(5) Å, c = 22.897(5) Å, $\alpha = \beta = \gamma$ = 90º, V = 8801(4) Å^3, Z = 4, μ = 22.544 mm^{-1}, Dc = 3.516 g·cm^{-3}, $F(000)$ = 8208.0, R_1 = 0.0593, wR_2 = 0.1589 (I > 2σ (I)), GOF = 1.006, T = 293(2) K. A total of 7915 data were measured. The data were corrected for absorption by the multi-scan. The H atoms have not been located, but were included into the formula directly. CCDC 919424.

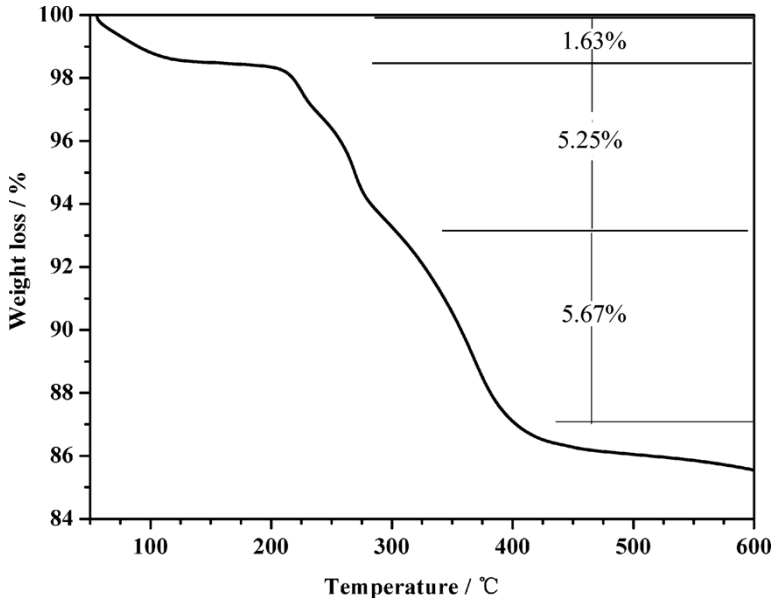

Fig. S1 TG curve of **1** measured under N_2 atmosphere with a heating rate of 10 °C·min^{-1}.

The weight loss of 1.63% (calcd 1.56%) below 200 °C was attributed to the loss of four lattice water molecules. The weight loss of 5.25% (calcd 5.87%) between 200–300 °C was attributed to the loss of all CH_3NHCH_3 organic cations, followed by the decomposition of **1a**. The observed experimental values are in approximate consistence with the theoretical values.

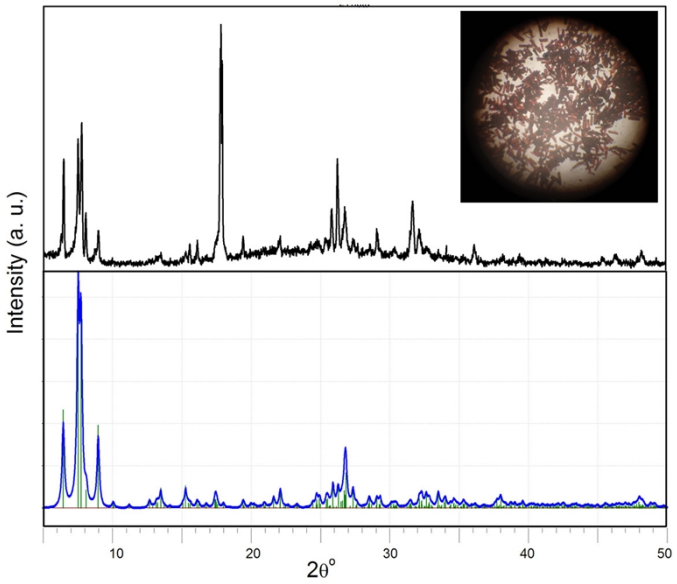

Fig. S2 The XRD pattern of the as-synthesized (top) and simulated pattern (bottom) of **1**. Inset: The photographs of compound **1** for XRD test.

The new simulated diffraction pattern from single-crystal XRD is obtained through the program 'Mercury' and 'Diamond'. The simulated/experimental XRD patterns (Fig. S2) match well in position, indicating the phase purity, which is confirmed by the photo (the inset of Fig. S2). The massive peak in the experimental data (around ca. 17.7 degrees) in two theta may be caused by the preferential orientation of (0, 2, 4) crystal plane in the measurement.

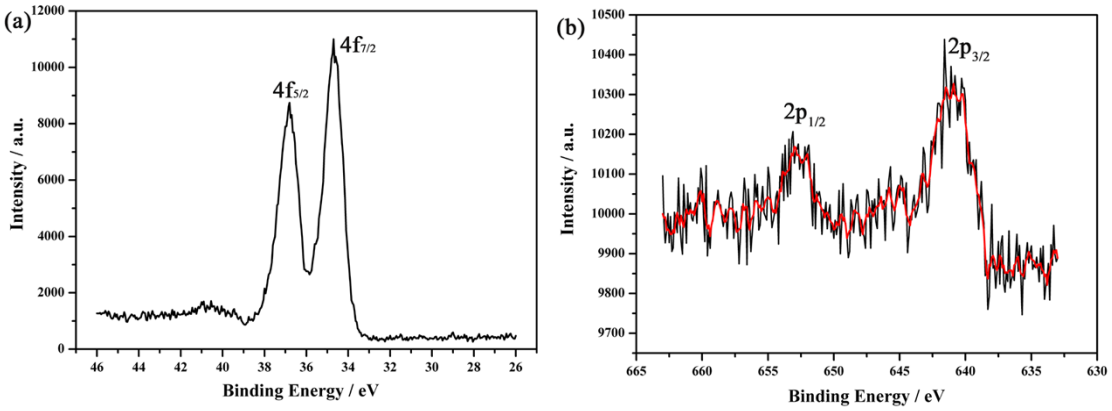

Fig. S3 XPS spectrum of compound **1**, (a) for W and (b) for Mn.

As shown in Fig. S3a, the XPS spectrum of **1** gives two peaks at 34.6 and 37.0 eV attributed to W^{6+} $4f_{7/2}$ and W^{6+} $4f_{5/2}$, respectively. [S1, S2] Fig. S3b shows two peaks at 641.5 and 653.0 eV, which can be ascribed to Mn $2p_{1/2}$ and $2p_{3/2}$. The distance between the two peaks is about 11.5 eV, which is consistant with the Mn^{3+} oxidation state.[S3]

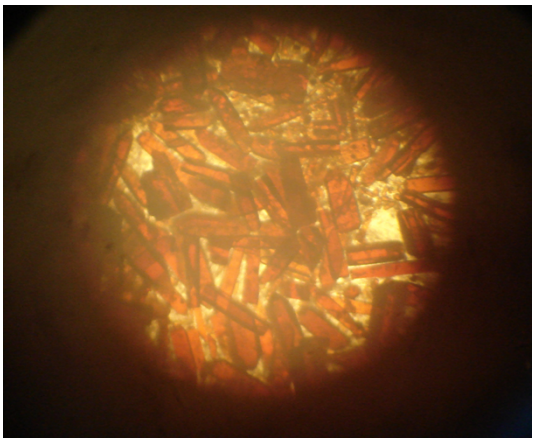

Fig. S4 The photographs of compound **1** showing the color of the crystal.

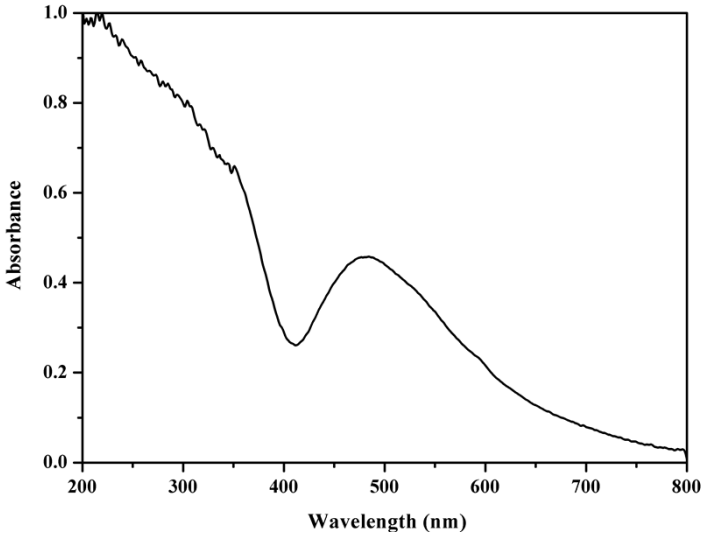

Fig. S5: UV-vis-NIR absorption spectrum of **1**.

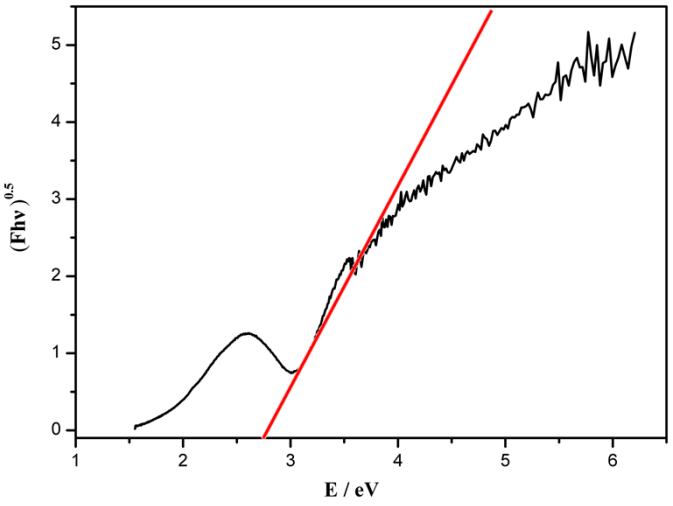

Fig. S6 The diffuse reflectance UV-vis-NIR spectra of $(Fh\nu)^{0.5}$ *vs.* energy (eV) of compound **1**. F = (1-R)*(1-R)/2R; A = log1/R.

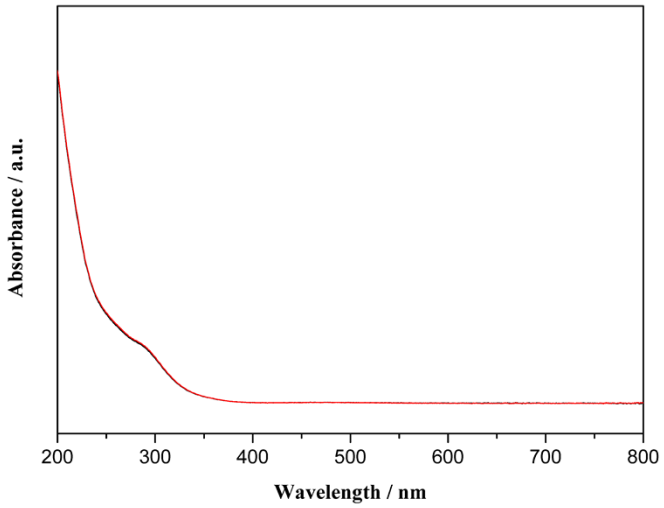

Fig. S7 UV-Vis spectra of compound **1** before (black) and after (red) the photocatalytic reactions with 100 mg compound **1**.

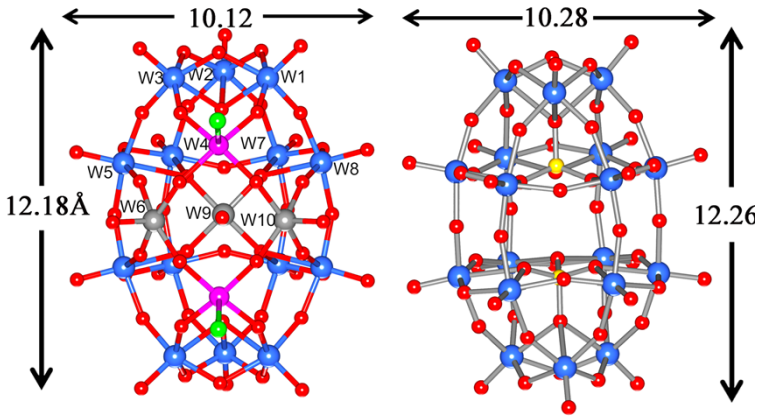

Fig. S8 Structural representations of the $\{Mn_2W_{17}\}$ (left) and $\{P_2W_{18}\}$ (right) for comparison. W: gray (in the penta-coordinated environment), blue (in the hexa-coordinated environment); P: yellow; Mn: purple; Cl: green; O: red.

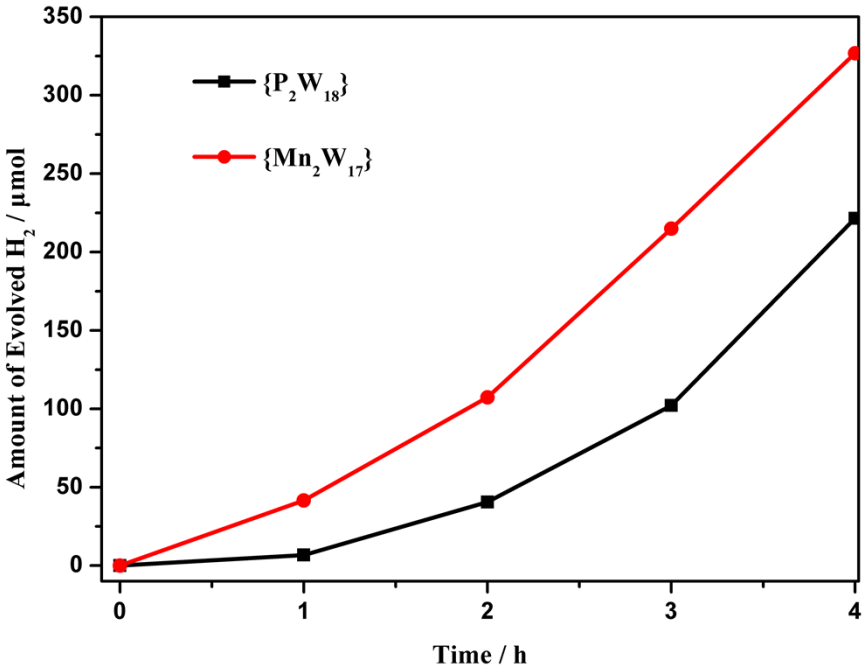

Fig. S9 Dependence of H_2 production on irradiation time with the use of **1** (red) and $\{P_2W_{18}\}$ (black) as photocatalysts. The experiments were performed in 100 mL of solution containing 10 mL CH_3OH, 90 mL water and 0.1 g catalysts.

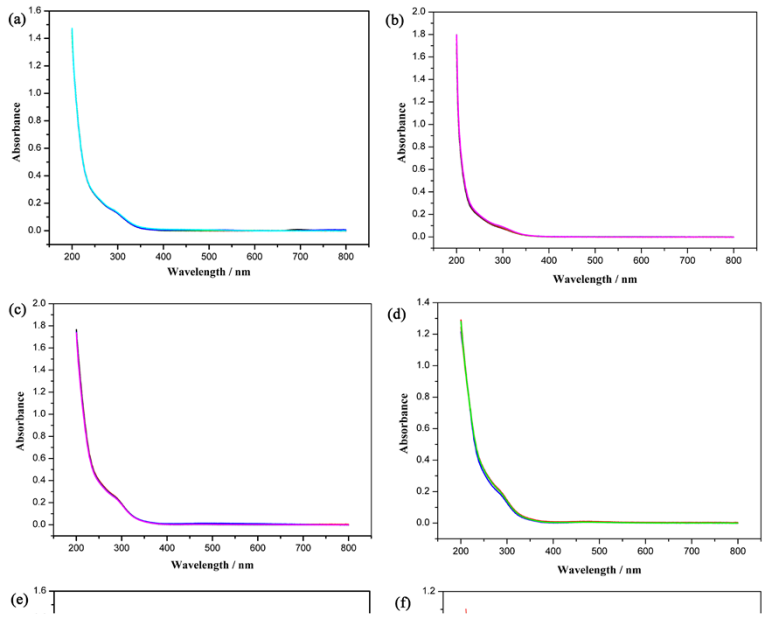

Fig. S10 The UV spectra of **1** in a varied pH aqueous solution (0.5 M H_2SO_4). The UV curves were detected per 24 hours for five times. (a): pH = 0.33; (b) pH = 1; (c) pH = 2; (d) pH = 3; (e) pH = 4; (f) in water.

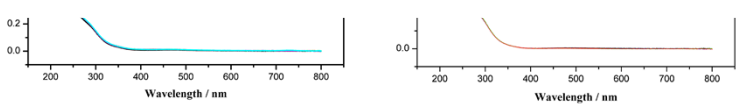

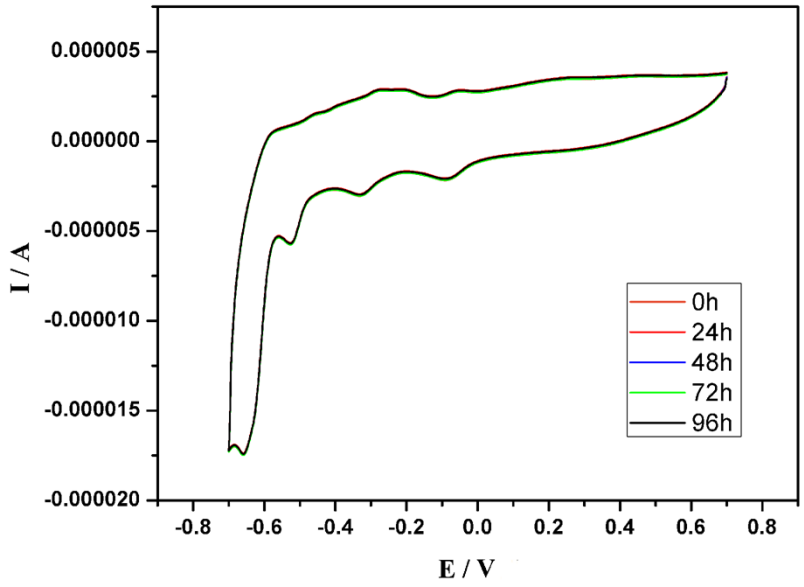

Fig. S11 Cyclic voltammograms of **1** were detected per 24 hours for five at a scan rate of 100 mV/s. Concentration of **1** was 4×10^{-5} M in 25 mL of pH 0.33 (0.5 M H_2SO_4) solution, the working electrode was glassy carbon (3 mm) and the reference electrode was Ag/AgCl.

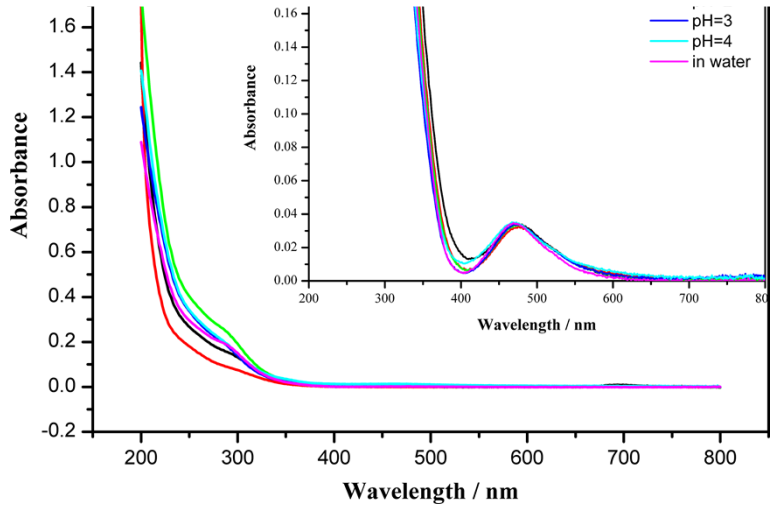

Fig. S12 The UV spectra of **1** in varied pH aqueous solution. Inset: The UV spectra of **1** in varied pH aqueous solution at high concentration. The peaks of Mn are located at about 476 nm.

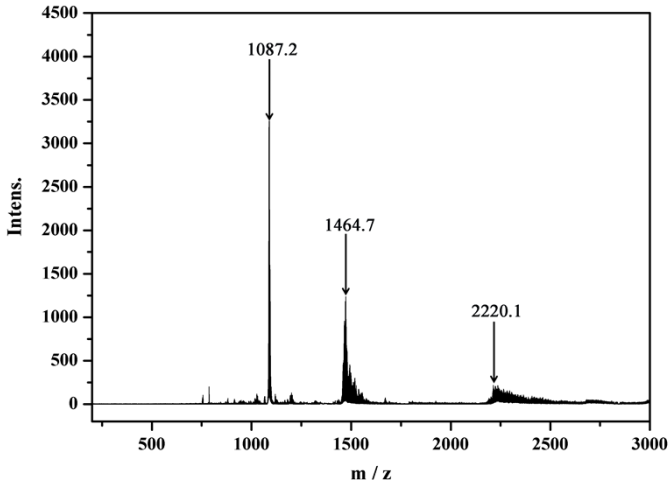

Fig. S13 ESI-MS of **1** in H_2O.

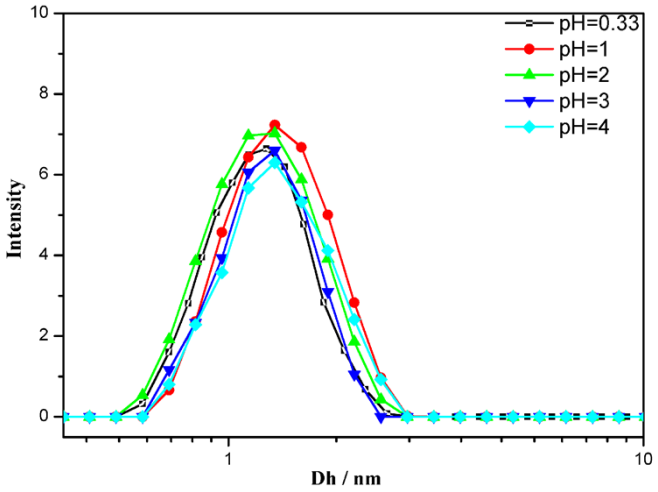

Fig. S14 DLS studies on **1** at different pH values.

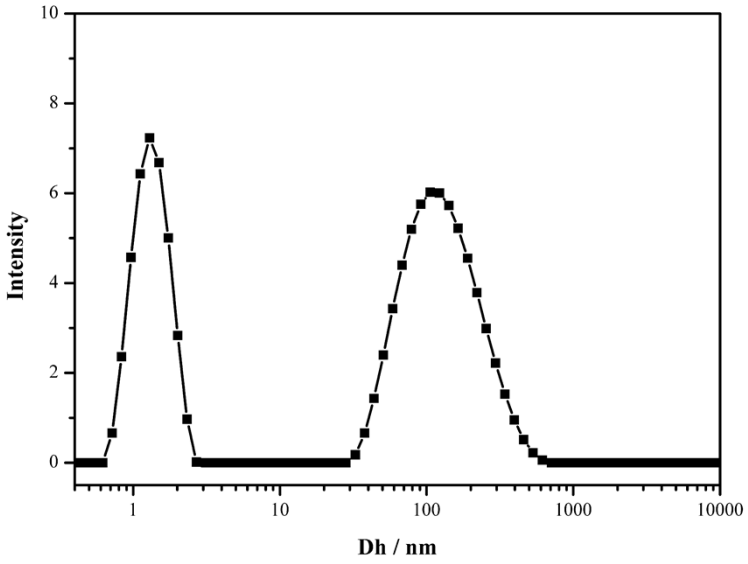

Fig. S15 Volume size distribution of particles of cluster **1** in solutions at pH 0.33 showing the formation of higher aggregation ~106 nm.

The ESI mass spectrum of compound **1** shows that the whole cluster is completely present and all the m/z values of the main peaks can be assigned to their different charge/cation states (Fig. S13). The strongest ones are centered at m/z 1087.2 and 1464.7 and have charges of −4 and −3, respectively. The other peak, which has an m/z value of 2220.1 and very low intensity compared to the other two, has a charge of −2. The assignments of peaks listed in the Supporting Information (Table S4) indicate that the polyoxoanion is stable in solution. Compound **1** was studied by dynamic light scattering (DLS) in solution with different pH values at 25 °C. The hydrodynamic radius Rh was consistent with the size of **1a**, remained unchanged when the pH varied between 0.33 and 4 (Fig. S14), and this indicates that the polyoxoanion is stable in solution. DLS experiments (Fig. S15) also pointed to the possibility that higher aggregations of **1a** may form, similar to the super macroions observed by Liu[S4], which is reminiscent of that reported by Cronin[S5].

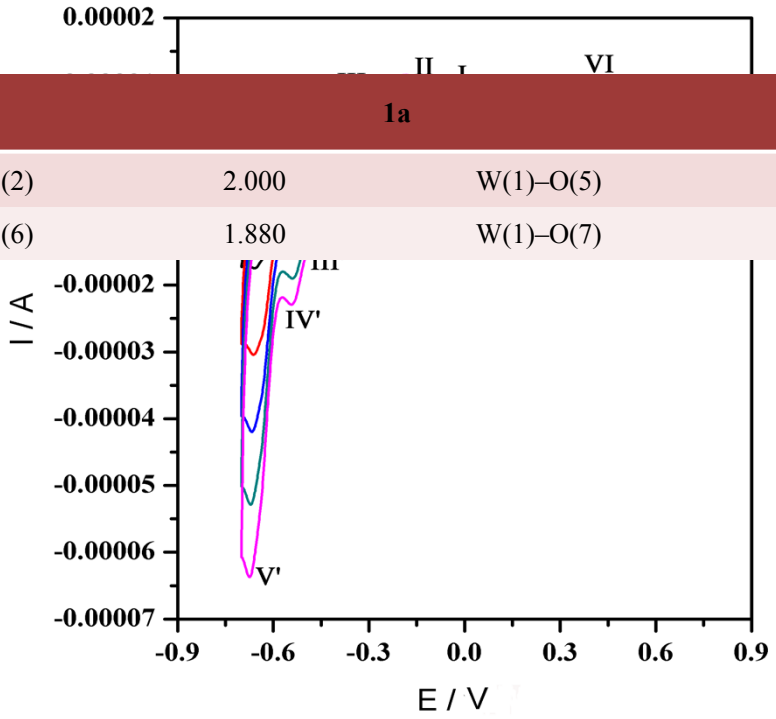

1a			
W(1)–O(2)	2.000	W(1)–O(5)	1.955
W(1)–O(6)	1.880	W(1)–O(7)	2.226

Fig. S16 Cyclic voltammograms of **1** in the potential region of +0.7 to –0.7 V at scan rates (from inner to outer) 100, 200, 300, 400 and 500 mV/s.

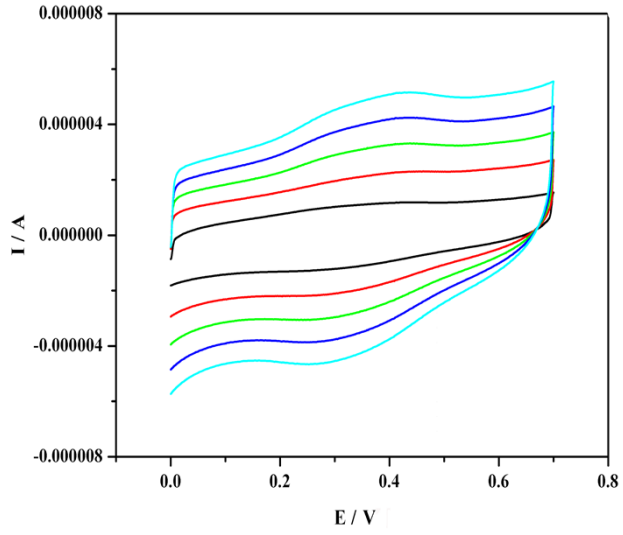

Fig. S17 Cyclic voltammograms of **1** in the potential region of 0 to +0.7 V at scan rates (from inner to outer) 100, 200, 300, 400 and 500 mV/s.

Table S1. Selected bond distances (Å) of **1a**.

W(1)–O(11)	1.864	W(1)–O(13)	1.785
W(2)–O(1)	1.782	W(2)–O(2)	1.913
W(2)–O(3)	1.919	W(2)–O(7)	2.273
W(2)–O(24)	1.923	W(2)–O(31)	1.894
W(3)–O(3)	1.994	W(3)–O(5)	1.889
W(3)–O(7)	2.240	W(3)–O(8)	1.709
W(3)–O(10)	1.885	W(3)–O(12)	1.834
W(4)–O(9)	2.288	W(4)–O(20)	1.926
W(4)–O(21)	1.712	W(4)–O(22)	1.917
W(4)–O(24)	1.913	W(4)–O(33)	1.883
W(5)–O(9)	2.354	W(5)–O(10)	1.918
W(5)–O(18)	1.902	W(5)–O(19)	1.712
W(5)–O(20)	1.925	W(5)–O(23)	1.899
W(6)–O(14)	1.815	W(6)–O(17)	1.790
W(6)–O(18)	1.923	W(7)–O(4)	1.923
W(7)–O(29)	2.312	W(7)–O(30)	1.867
W(7)–O(31)	1.930	W(7)–O(32)	1.703
W(7)–O(33)	1.942	W(8)–O(6)	1.925
W(8)–O(26)	1.823	W(8)–O(27)	1.920
W(8)–O(28)	1.708	W(8)–O(29)	2.306
W(8)–O(30)	1.960	W(9)–O(9)	1.910
W(9)–O(25)	1.790	W(9)–O(29)	1.904
W(10)–O(15)	1.849	W(10)–O(16)	1.785
W(10)–O(26)	1.985	Mn(1)–O(11)	1.857
Mn(1)–O(12)	1.880	Mn(1)–O(14)	1.905
Mn(1)–O(15)	1.872	Mn(1)–Cl(1)	2.500

Table S2. The BVS calculation result of all the metal atoms in **1**.

Code	**Bond Valence**	**Code**	**Bond Valence**
W1	5.823	W7	6.156

W2	5.876	W8	6.258
W3	6.404	W9	5.877
W4	6.191	W10	5.497
W5	6.114	Mn1	3.267
W6	6.012		

Table S3. The BVS calculation result of all the oxygen atoms in **1**.

Oxygen Code	Bond Valence	Oxygen Code	Bond Valence	Oxygen Code	Bond Valence
O1	1.440	O12	1.974	O23	2.100
O2	1.810	O13	1.429	O24	1.995
O3	1.807	O14	1.993	O25	1.410
O4	1.968	O15	1.941	O26	2.121
O5	1.981	O16	1.429	O27	1.984
O6	2.084	O17	1.410	O28	1.759
O7	1.234	O18	2.025	O29	1.729
O8	1.754	O19	1.740	O30	2.035
O9	1.693	O20	1.955	O31	2.029
O10	2.087	O21	1.740	O32	1.783
O11	1.923	O22	2.002	O33	2.031

Table S4. Assignment of peaks in negative mode Mass spectrum of cluster **1**.

Peak code	Observed m/z	Envelope Assignment	Molecular mass	Calculated m/z
1	1087.2917	$\{(CH_3NH_2CH_3)_2H_6[(WO_5)_3W_{14}Mn_2O_{44}Cl_2]\}^{4-}$	4358.2571	1087.0643
2	1464.6492	$\{(CH_3NH_2CH_3)_3H_6[(WO_5)_3W_{14}Mn_2O_{44}Cl_2]\}^{3-}$	4394.3487	1464.7829
3	2220.0526	$\{(CH_3NH_2CH_3)_4H_6[(WO_5)_3W_{14}Mn_2O_{44}Cl_2]\}^{2-}$	4440.4404	2220.2202

References

[S1] Y. Wang, L. N. Xiao, H. Ding, F. Q. Wu, L. Ye, T. G. Wang, S. Y. Shi, X. B. Cui, J. Q. Xu and D. F. Zheng, *Inorg. Chem. Commun.*, 2010, **13**, 1184.

[S2] W. C. Chen, H. L. Li, X. L. Wang, K. Z. Shao, Z. M. Su and E. B. Wang, *Chem.–Eur. J.* 2013, **19**, 11007.

[S3] Q. Wu, Y. G. Li, Y. H. Wang, E. B. Wang,. Z. M. Zhang and R. Clérac, *Inorg. Chem.*, 2009, **48**, 1606.

[S4] T. Liu, *J. Am. Chem. Soc.* 2003, **125**, 312.

[S5] C. P. Pradeep, D. L. Long, C. Streb, L. Cronin, *J. Am. Chem. Soc.* 2008, **130**, 14947.